Gynecologic Oncology 156 (2020) 222–232

Contents lists available at ScienceDirect

Gynecologic Oncology

journal homepage: www.elsevier.com/locate/ygyno

An autologous humanized patient-derived-xenograft platform to evaluate immunotherapy in ovarian cancer

Sarah B. Gitto [a, b, c], Hyoung Kim [a], Stavros Rafail [a], Dalia K. Omran [a, c], Sergey Medvedev [a], Yasuto Kinose [a], Alba Rodriguez-Garcia [a, b, c], Ahron J. Flowers [a], Haineng Xu [a], Lauren E. Schwartz [c], Daniel J. Powell Jr. [a, b, c, **, 1], Fiona Simpkins [a, *, 1]

[a] Ovarian Cancer Research Center, Division of Gynecology Oncology, Department of Obstetrics and Gynecology, Perelman School of Medicine, University of Pennsylvania, Philadelphia, PA, 19104, USA
[b] Center for Cellular Immunotherapies, University of Pennsylvania, Philadelphia, PA, 19104, USA
[c] Department of Pathology and Laboratory Medicine, Abramson Cancer Center, Perelman School of Medicine, University of Pennsylvania, Philadelphia, PA, 19104, USA

HIGHLIGHTS

- Patient-matched orthotopic PDX/TIL models were developed and validated.
- TILs with autologous tumor reactivity were successfully expanded from donor HGSOC for infusion.
- TILs co-cultured with autologous tumor cells exhibited HLA-dependent IFNγ production and activation.
- Combination TILs and anti-PD-1 significantly increased patient-matched tumor cell lysis and increased survival *in vivo.*

ARTICLE INFO

Article history:
Received 9 March 2019
Received in revised form
9 October 2019
Accepted 9 October 2019
Available online 7 December 2019

Keywords:
Ovarian cancer
Patient derived xenograft
Tumor infiltrating lymphocytes
Anti-PD-1

ABSTRACT

Objective: The aim of this study was to "humanize" ovarian cancer patient-derived xenograft (PDX) models by autologous transfer of patient-matched tumor infiltrating lymphocytes (TILs) to evaluate immunotherapies.
Methods: Orthotopic high-grade serous ovarian cancer (HGSOC) PDX models were established from three patient donors. Models were molecularly and histologically validated by immunohistochemistry. TILs were expanded from donor tumors using a rapid expansion protocol. *Ex vivo* TIL and tumor co-cultures were performed to validate TIL reactivity against patient-matched autologous tumor cells. Expression of TIL activation markers and cytokine secretion was quantitated by flow cytometry and ELISA. As proof of concept, the efficacy of anti-PD-1 monotherapy was tested in autologous TIL/tumor HGSOC PDX models.
Results: Evaluation of T-cell activation in autologous TIL/tumor co-cultures resulted in an increase in HLA-dependent IFNγ production and T-cell activation. In response to increased IFNγ production, tumor cell expression of PD-L1 was increased. Addition of anti-PD-1 antibody to TIL/tumor co-cultures increased autologous tumor lysis in a *CCNE1* amplified model. Orthotopic HGSOC PDX models from parallel patient-matched tumors maintained their original morphology and molecular marker profile. Autologous tumor-reactive TIL administration in patient-matched PDX models resulted in reduced tumor burden and increased survival, in groups that also received anti-PD-1 therapy.
Conclusions: This study validates a novel, clinically relevant model system for *in vivo* testing of immunomodulating therapeutic strategies for ovarian cancer, and provides a unique platform for assessing patient-specific T-cell response to immunotherapy.

* Corresponding author. University of Pennsylvania, 3400 Civic Center Blvd, South Tower, Suite 10-176, Philadelphia, PA, 19104-5156, USA..
** Corresponding author. University of Pennsylvania, 3400 Civic Center Blvd, Bldg 421, Smilow CTR, Office 8-103, Philadelphia, PA, 19104-5156, USA.
E-mail addresses: Sarah.Gitto@pennmedicine.upenn.edu (S.B. Gitto), hyoungk@pennmedicine.upenn.edu (H. Kim), psil@hotmail.com (S. Rafail), domran@pennmedicine.upenn.edu (D.K. Omran), medvedev@pennmedicine.upenn.edu (S. Medvedev), yasutok@pennmedicine.upenn.edu (Y. Kinose), albarod@pennmedicine.upenn.edu (A. Rodriguez-Garcia), aflow@pennmedicine.upenn.edu (A.J. Flowers), haineng@pennmedicine.upenn.edu (H. Xu), Lauren.Schwartz@uphs.upenn.edu (L.E. Schwartz), poda@pennmedicine.upenn.edu (D.J. Powell), Fiona.Simpkins@pennmedicine.upenn.edu (F. Simpkins).
[1] Authors contributed equally.

https://doi.org/10.1016/j.ygyno.2019.10.011
0090-8258/

1. Introduction

Ovarian cancer is the fifth leading cause of cancer related deaths among women, resulting in nearly 14,000 deaths in the U.S. annually, with the majority of cases demonstrating high-grade serous histology [1]. Despite high response rates to aggressive surgical resection and first-line carboplatin–taxane chemotherapy, recurrence occurs in nearly 80% of cases. Patients with recurrent high-grade serous ovarian cancer (HGSOC) ultimately acquire platinum-resistance and succumb from disease [2,3]. For approximately 50% of HGSOCs, defects in homologous recombination (HR; e.g. *BRCA1/2*) cause sensitivity to PARP inhibitors (PARPi) [4,5], but complete response rates are low (2–9%) with partial responses being more common in the recurrent setting (35%) [6,7]. The other 50% of HGSOCs are HR-proficient, and frequently exhibit increased Cyclin E expression (~40%) either by *CCNE1* gene amplification (20%) or *CCNE1* copy-number gain (34%). Tumors with *CCNE1* amplification are associated with poor overall survival and platinum-resistance [8–11]. Despite recent advances exploiting the genetics of ovarian cancer, most recurrent HGSOC ultimately develops drug resistance. Accordingly, alternative therapeutic strategies that increase complete and durable responses or delay death in HGSOC are needed.

In HGSOC, improved progression free survival and overall survival is associated with increased intraepithelial tumor-infiltrating-lymphocytes (TILs), in particular T-cells ($CD8^+$), which occurs in about 55% of cases [12]. In spite of clear evidence of endogenous immunity in HGSOC [13], tumor cells employ multiple mechanisms to evade TIL activity, including up-regulation of immunosuppressive checkpoint molecules such as programmed death-ligand 1 (PD-L1). HGSOC cells increase PD-L1 expression in the presence of activated cytotoxic T-cells [14,15] and in response to interferon gamma (IFNγ) exposure [15]. T-cells themselves upregulate the expression of programmed cell death protein 1 (PD-1) upon activation. Interaction of T-cell surface PD-1 with PD-L1 on tumor cells suppresses T-cell signaling, cytokine production, and proliferation [14,16,17]. Blockade of the PD-1/PD-L1 interaction can result in the restoration of T-cell activity against tumors, enhancing the therapeutic potential of the immune system.

Various PD-1 and PD-L1 antagonists are FDA approved for many types of cancer [18–20]. Trial results for PD-1 or PD-L1 inhibitors as monotherapy in HGSOC have been disappointing with overall response rates of about 10% [20,21], but some durable, complete responses have been documented. Our ability to predict which patients will benefit from this therapy is limited, and combinations will likely be required [22]. Combination immune checkpoint inhibition, by blocking PD-1 (e.g. nivolumab) and CTLA4 (e.g. ipilimumab), was tested in a phase II randomized clinical trial (NRG-GY003) and showed an increased overall response rate (31.4% vs 12.2) and doubling of progression free survival (3.9 vs. 2.0 months) compared to single-agent anti-PD-1 therapy [23]. Nevertheless, strategies are required to determine the optimal drug schedule, and sequence for these immunomodulating therapies. Predictive biomarkers of response are also needed in order to preselect patients who will benefit from these therapies.

Development of *in vivo* model systems that allow for patient-specific preclinical testing of such strategies would potentially facilitate optimization of immunotherapies in HGSOC. In order to develop clinically relevant models of HGSOC for testing therapeutic strategies, we and others have applied patient-derived xenograft (PDX) models. These models recapitulate the biology of the original patient tumor, mimic drug response to that of the patient, and can better recapitulate the tumor microenvironment than historic cell line models for HGSOC [24–26]. Preclinical studies using PDX models developed from patient tumors, performed in parallel to clinical trials, have shown that PDX models reliably reproduce clinical outcomes [27,28]. However, these models of engrafted human tumors generally rely on immunodeficient mice that lack a human immune system, making it difficult to test immunomodulating therapies *in vivo*. To overcome this obstacle, humanization of xenograft and PDX models using healthy donor peripheral blood mononuclear cells (PBMCs) and hematopoietic stem cells (HSCs) have been created [29], however, these models lack an autologous adaptive immune response that has been primed against patient-specific tumor antigens.

We have now developed a "humanized" orthotopic PDX platform for HGSOC by performing autologous tumor-reactive TIL transfer, using T cells derived from the same patient's tumor, in newly established orthotopic PDX models to create a platform for assessing patient-specific T-cell responses to immune therapy *in vivo*. We validated the utility of this novel preclinical patient-matched TIL/PDX model by testing both the impact of endogenous T-cell immunity and immune enhancing therapies, such as PD-1 inhibitors, on HGSOC progression. Our results demonstrate proof of concept for the humanized orthotopic HGSOC PDX platform as a valuable preclinical *in vivo* model system of host T-cell/tumor interaction that allows for assessment of patient-specific endogenous T-cell function, and for the testing of immune modulating agents and combination strategies *in vivo*.

2. Methods and materials

2.1. DNA sequencing and mutational analysis of patient tumors

Somatic mutation screening and copy number alteration analysis was performed on original patient tumors and PDX models using a custom designed targeted massively parallel sequencing protocol as previously described [24].

2.2. Autologous TIL-PDX models

Patient tumors were acquired from the Hospital of the University of Pennsylvania in accordance with IRB (#702679). NOD-SCID IL2Rγ$^{-/-}$ (NSG) mice were purchased from the Stem Cell Xenograft Core at the University of Pennsylvania (UPENN) and housed in accordance to UPENN IACUC protocols (#806002). PDX models were generated as previously described [24]. In short, about three ~3 mm^3 tumor chunks were sutured onto the fallopian tube/ovaries of 5 to 8-week-old female NSG mice, and 5–10 μl of Matrigel was placed over the transplant. When the tumor reached approximately 700–1,000 mm^3, the tumor was excised and small tumor chunks again transplanted in a similar fashion for expansion (MP2). MP2 tumor was then used for preclinical studies. For all pre-clinical studies, mice were monitored daily, weights and condition scores were collected weekly, and tumor volume was measured by ultrasound weekly. For WO-12 and WO-19 studies, when the tumor grew to 70–100 mm^3, mice were randomized to treatment groups. Mice were injected with 1×10^7 autologous TILs i.p. weekly, and the following day with 10 mg/kg α-PD-1 or PBS (vehicle) i.p. This regimen was repeated for up to six weeks. For the WO-6 study, tumor was transplanted then 4 days later, 1×10^7 were TILs were injected followed by bi-weekly 10 mg/kg α-PD-1 or IgG4 i.p. administration. When the tumor volume reached >1000 mm^3, mice were euthanized according to IACUC guidelines.

2.3. Histological analysis

Upon euthanasia, tumors were harvested and fixed in 10% neutral buffered formalin. Tissues were dehydrated in graded ethanol solutions, cleared in xylene, then embedded in paraffin. Blocks were cut into 5 μm sections and stained using the DAKO CoverStainer for H&E (Agilent, Santa Clara, CA).

Immunohistochemisty was performed using the DAKO EnVision Plus System with the DAKO Autostainer Plus Immunostainer, or the Leica Bond-IIITM with the Bond Polymer Refine Detection System. Then the tissue was dehydrated and antigen retrieval was optimized using sodium citrate, pH 6.0 or EDTA, pH 9.0. Primary antibodies used for this study included CD3, p53, WT1 (DAKO), CD8 (Invitrogen), CD4 (Abcam), PD-L1, PD-1 (Cell Signaling), Pax8 (Cell Marque), and AE1/3 (Leica). Images were taken using a Leica DM 2000 microscope. For quantification of $CD3^+$ T-cell infiltration, the average number of $CD3^+$ T-cells per mouse was calculated from 40 to 60 10x fields.

2.4. Establishing primary WO-12 tumor cultures

Tumor was obtained from patients at the time of ovarian cancer debulking surgeries (IRB #702679). Tumor was minced, digested with collagenase and then further dissociated using a 40 μm cell strainer. Cells were pelleted then resuspened in OCMI media (Live Tumor Culture Core, U. Miami) [34] supplemented with 25 μg/ml cholera toxin (Calbiochem) [30]. Cells were grown on primeria tissue culture flasks (Corning) in hypoxic conditions until required for *in vitro* experiments.

2.5. Tumor infiltrating T-cell isolation and rapid expansion

Patient-matched frozen tumor samples were obtained from the PENN Ovarian Cancer Research Center Biotrust Collection (https://www.med.upenn.edu/OCRCBioTrust/). Specimens were enzymatically digested overnight at 37 °C with a collagenase (200 μg/mL) and DNAse (30U) solution in RPMI [13]. Tumor digest was incubated overnight with recombinant IL-7 and IL-15. Pan $CD3^+$ cells were isolated by the EasySep Human T Cell Enrichmnet Kit per manufacturer's instructions (Stemcell Technologies). KT64-BBL APCs were grown overnight in serum-free AIM-V media (Gibco) then irradiated at 10,000 rads using the X-RAD 320 ix biological irradiator (Precision X-Ray, North Bradford, CT). APCs were preloaded with 0.5 μg/10^6 cells anti-CD3 (OKT-3;Miltenyi Biotec, Auburn, CA) and CD28 (15E8; Miltenyi Biotec) antibodies for 30 min at 4 °C. Cells were washed twice with serum free AIM-V, then resuspended in complete culture medium [31]. Isolated T-cells were co-cultured with APCs overnight in complete culture media. T-cells were diluted to 6×10^5 cells/mL and supplemented with 600 IU/mL Proleukin the next day and every other day after (Prometheus Laboratories, San Diego, CA). After 12–14 days of expansion, T-cells were cryogenically preserved in FBS+10% DMSO until use in experiments.

2.6. TIL activation assays

Freshly dissociated WO-19 and WO-6 PDX tumor cells, or WO-12 primary cells were co-cultured with patient-matched TILs at 37 °C. HLA block or isotype (BioLegend) were added and supernatants were collected after 24 h for ELISA (BioLegend). Cell pellets were stained with Live/Dead Fixable Aqua (Invitrogen) or Violet (BioLegend) viability dye, washed, and then stained with CD45, PD-1, PD-L1, EPCAM (BioLegend), CD8 (BD Biosciences), and CD69 (Invitrogen) antibodies. An IFNγ Secretion Assay was performed with patient-matched WO-12 TILs and tumor cells per protocol (Miltenyi Biotec). Prior to plating, WO-12 TILs were labeled with IFNγ Catch Reagent for 5 min, plated at a 1:1 effector-target ratio, and then incubated for 6 h at 37 °C. Cell Stimulation Cocktail (PMA and ionomycin; eBiosciences) was used as a positive control. Samples were analyzed by flow cytometry (LRSFortessa, BD Biosciences) and FlowJo Software.

2.7. TIL mediated cytolysis

To determine tumor lysis by patient-matched autologous TILs, co-cultures were analyzed on the xCELLigence Real-Time Cell Analysis (RTCA) multiplate system (ACEA Biosciences, San Diego, CA). Dissociated WO-19 PDX tumor cells or WO-12 primary cells were plated (ACEA Biosciences). Cell growth was dynamically monitored using RT-CES system (ACEA Biosciences) for 24–48 h. TILs at a 1:1 tumor to target ratio with or without anti-PD-1 were added (10 μg/mL) to tumor cell cultures.

2.8. Statistical analysis

When appropriate, results were reported as mean ± SD or mean ± SEM. Data were analyzed using one-way ANOVA with Dunnett's multiple comparisons post-hoc test, or two-way ANOVA with Tukey's multiple comparisons post-hoc test, or unpaired Students T-test. Additionally, *in vivo* survival studies were analyzed by Log-rank test and tumor volume over time was analyzed by area under the curve followed by a one-way ANOVA. Statistical significance was set at $^*<0.05$, $^{**}<0.01$, $^{***}< 0.001$, $^{****}<0.0001$ (GraphPad Prism, La Jolla, CA). *In vitro* experiments were replicated at least three times.

3. Results

3.1. Development of PDX models for autologous humanization

PDX models recapitulate the characteristics of a patient's original tumor, but lack the immune component known to control HGSOC progression [24,26,32,33]. We therefore sought to humanize PDX models by transplanting immune-deficient mice with patient ovarian tumors and infusing matched autologous-expanded tumor infiltrating lymphocytes (TILs), which would enable the evaluation of host immunity on cancer progression and the impact of immunotherapy (Fig. 1). Fresh ovarian tumor was transplanted to the ovaries of mice generating orthotopic PDX models as previously described [24]. In parallel, fresh tumor collected at the time of surgery was enzymatically dissociated and banked to establish primary tumor cultures for *in vitro* assays. TILs were isolated and expanded for *in vitro* co-culture assays and *in vivo* administration.

PDX tumor models and *ex vivo* TIL cultures were developed from three patient donors. The clinical and next generation sequencing data from the patient's tumor are outlined in Table 1. Histolgies were confirmed by a gynecologic pathologist. Patient tumor WO-12 and WO-6 were platinum-sensitive, whereas patient tumor WO-19 was platinum-resistant. The WO-19 tumor exhibited a *CCNE1* amplification [9,10,34]. The patients' original tumor morphology and expression of HGSOC markers, including paired box gene 8 (Pax8), p53, cytokeratin AE1/3, and Wilms' Tumor 1 (WT1), was well maintained in PDX tumor models (Fig. S1). *Ex vivo* TIL cultures were also established for a previously developed and characterized PDX model, WO-6 [24]. This model is *BRCA1* mutant ($BRCA1^{mut}$) and was sensitive to platinum therapy. Patient tumors were tested for DNA mismatch repair proteins: MLH1, MSH2, MSH6, and PMS2. Expression was retained in the all tumors, suggesting intact mismatch repair mechanisms.

3.2. Variation of T-cell populations and PD-1/PL-L1 axis in PDX models

One main advantage of PDX models is that they retain the tumor heterogeneity and to some degree, the stromal and immune compartment of the original tumor [24,26,32,33]. To evaluate the PDX immune microenvironment, PDX and original patient tumors were characterized for T-cell infiltration, as well as expression of

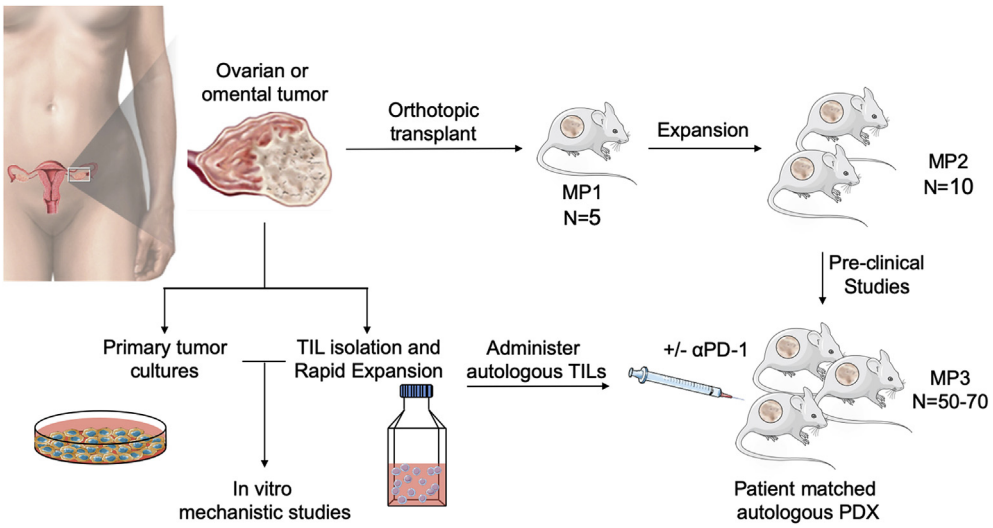

Fig. 1. Patient-matched autologous PDX/TILs model development. HGSOC tumor tissue collected at the time of debulking surgery, from either the ovary or the omentum, was used to both establish orthotopic PDX models, and to establish *ex vivo* patient tumor and tumor infiltrating lymphocyte (TIL) cultures. To establish PDX models, fresh tumor chunks (~3 mm^3 pieces), were transplanted onto the fallopian tube/ovary of five immunodeficient NOD.Cg-Prkdc^{scid}Il2rg^{tm1Wjl}/SzJl (NSG) mice (mouse passage 1; MP1). When the tumor volume reached ~700–1,000 mm^3, the tumor was excised and re-transplanted for expansion (MP2), and then again for pre-clinical trials (MP3). Tumor associated lymphocytes from dissociated primary tumors were isolated and expanded for *ex vivo* mechanistic studies, or for *in vivo* pre-clinical studies using patient-matched PDX/TIL models.

Table 1
Clinical and sequencing data for orthotopic HGSOC PDX tumors.

Patient Donor	Specimen	Stage	Pathology	Biopsy Time	Platinum Sensitivity	Pathogenic Mutations/Amplification	MMR status
WO-12-1	Omental Tumor	IV	HGSOC	1° CRS	Sensitive	TP53 c.983delT	Retained
WO-19-1	Ovarian Tumor	III_C	HGSOC	2° CRS	Resistant	TP53 c.C1024T *CCNE1* amp	Retained
WO-6	Omental Tumor	III_C	Mixed HGSOC with clear cell	2° CRS	Sensitive	TP53 c.G733A BRCA1 c.5266dupC	Retained

Abbreviations: amp, amplification; CRS, cytoreductive surgery; HGSOC, high-grade serous ovarian cancer; MMR, mismatch repair.

PD-1 and PD-L1 (Fig. 2A and B). WO-12 patient and PDX tumors had low expression of PD-1 (Fig. 2B), and were negative for PD-L1 by Immunohistochemistry (not shown). Human T-cell analysis determined that both patient tumors WO-12 and WO-19, had substantial infiltration of $CD4^+$ and $CD8^+$ T-cell populations, with an increased ratio of $CD4^+$ cells. After two mouse passages, the WO-12 PDX model was virtually void of originating T-cells. In contrast, WO-19 tumor model retained $CD4^+$ T-cells, albeit at lower levels, and these cells co-localize with regions that also express PD-1 (Fig. 2B). Four additional HGSOC models (WO-3, WO-6, WO-7, and WO-18) were characterized for CD3, CD8 and $CD8^+$ T-cells and the cell number per field was quantified. Results indicate two model retained, to some extent, T-cells after two serial mouse passages, whereas all other models were lacking all CD4 and CD8 T-cells (Fig. S2). This suggests that some early passage orthotopic ovarian PDX models can partially maintain the compartments of the original patient immune-microenvironment initially but is significantly reduced after multiple passages.

3.3. Expansion and subset characterization of TILs from human HGSOC tumors

In order to humanize the orthotopic HGSOC PDX model, autologous patient-matched TILs were isolated and expanded for future administration. The methodologies applied for TIL isolation from patient tumor homogenate and expansion are outlined in Fig. 3A. Enzymatically digested tumors were initially cultured with Interleukin (IL)-7 and IL-15 to maintain and initiate the expansion of $CD3^+$ T-cells, including the preferential expansion of the tumor-reactive TIL subset [31]. Growth rate was measured throughout the culture, and after 12–14 days in culture, 8- to 10-fold expansion of TILs was achieved (Fig. 3B and F). WO-12 TIL cultures consisted of 90% $CD3^+$ cells with 71.5% $CD8^+CD3^+$ T-cells, and WO-19 TIL cultures had nearly 100% T-cell purity with 93.4% being $CD8^+CD3^+$ T-cells (Fig. 3B and F). In summary, expansion resulted in enrichment of the adaptive immune system, primarily cytotoxic and helper T cells to assess patient-specific T-cell responses.

3.4. TILs are reactive against patient-matched tumor cells

To assess whether expanded TILs were reactive against patient-matched tumor cells, *ex vivo* co-culture assays were performed, followed by analyses of T-cell cytokine secretion and expression of cell surface activation markers. WO-12 TILs co-cultured with WO-12 primary tumor cells resulted in increased frequencies of IFNγ+ T-cells by flow cytometry based IFNγ-capture assay, indicating T-cell activation (Fig. 3C). Pan-blockade of human leukocyte antigen (HLA) using MHC class I antibodies did not significantly reduce T-cell activation, suggesting a role for $CD4^+$ cells in the response against autologous tumor cells. Here, the addition of PMA/I (Phorbol-Myristate-Acitate and Ionamycin) is a positive control for T-cell activation and IFNγ secretion. Co-culture also resulted in increased frequencies of T-cells expressing the activation markers CD69 and PD-1 (Fig. 3D). Co-culture of WO-19 TILs with WO-19 tumor homogenate resulted in a significant increase in secreted IFNγ (Fig. 3G, $p < 0.0001$). Similar to WO-12, WO-19 co-culture resulted in an increase in the frequency of T-cells expressing CD69 and PD-1 (Fig. 3H). Blocking with MHC class I neutralizing antibodies resulted in reduction of both IFNγ and activation markers, signifying that activation of TILs is dependant upon interaction with peptide/HLA complexes, as shown previously [13].

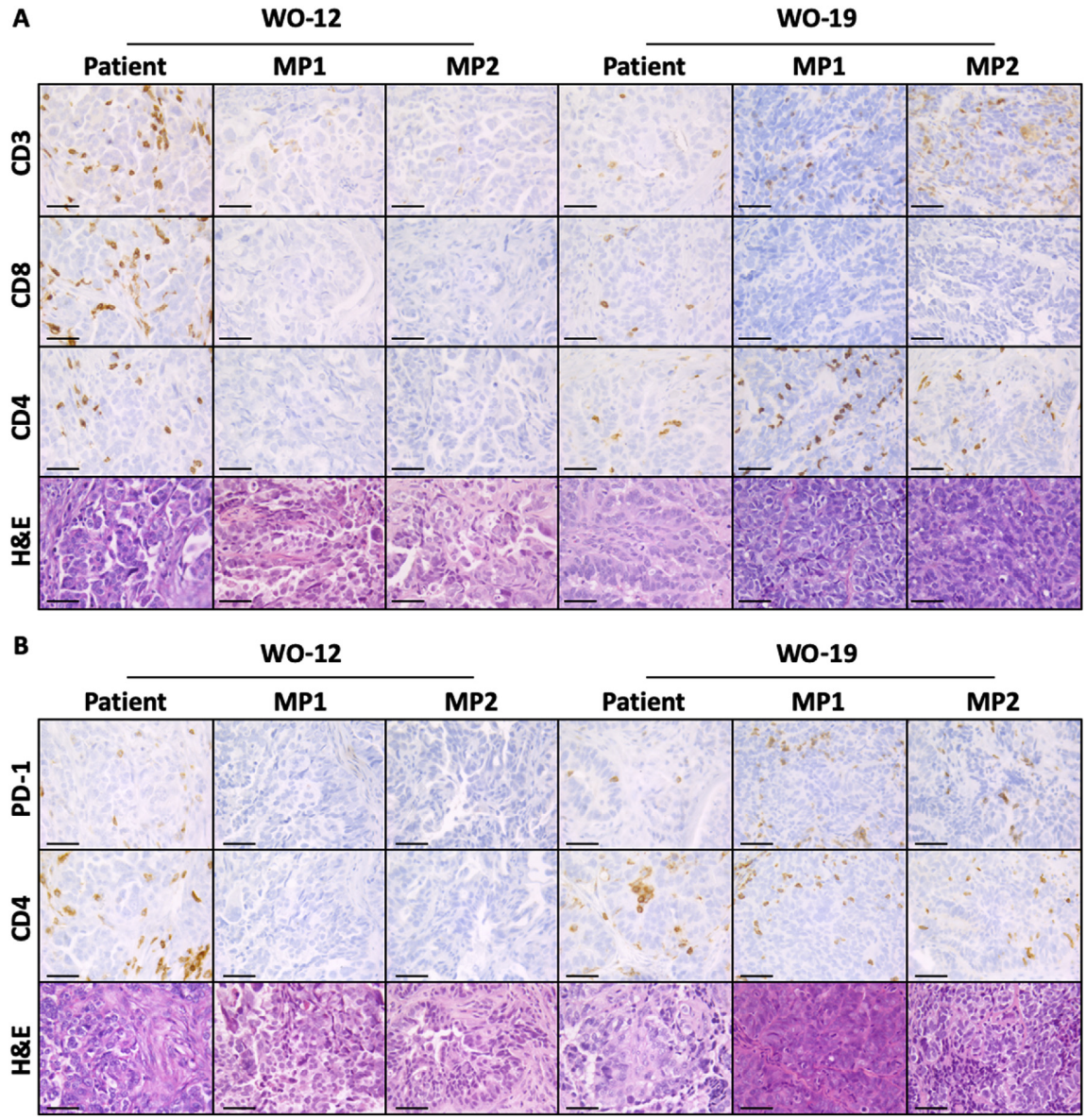

Fig. 2. Characterization of T-cell populations and PD-1/PD-L1 axis in PDX models. Histology of HGSOC malignancies from the original patient tumors and PDX tumors (MP1 and MP2) from donors WO-12 and WO-19. (A) Immunohistochemistry for CD3, CD8, CD4, and H&E stains are shown. Representative images were taken at 40x magnification and the scale bar denotes 50 μm. (B) Immunohistochemistry for PD-1, CD4 and H&E stains are shown. Representative images were taken at 40x magnification and the scale bar denotes 50 μm.

The interaction of T-cell surface PD-1 with PD-L1 on tumor cells results in inhibition of T-cell signaling, cytokine production and proliferation [16,17]. IFNγ can also upregulate PD-L1 expression on tumor cells, thereby dampening effector T-cell surveillance by adaptive resistance. Flow cytometry was performed to evaluate PD-L1 expression by patient tumor cells before and after exposure to tumor-reactive TILs. PD-L1 expression on $CD45^{-}EPCAM^{+}$ tumor cells was low at baseline but increased for both donors when cultured with their respective patient-matched TILs (Fig. 3E and I), thus providing rational for assessing the impact of PD-1 checkpoint blockade on the cytolytic function of autologous TILs.

3.5. *Anti-PD-1 increases cytotoxicity of autologous TILs against patient-matched tumor cells*

To determine if autologous TILs have cytolytic activity against patient-matched tumor cells, co-cultures were analyzed for tumor lysis in real time using xCELLigence technology. Tumor cells were plated and TILs were added to the culture the following day. Tumor cell lysis was longitudinally monitored for up to 4 days. WO-12 TILs modestly lysed autologous tumor cells. (Fig. 4**, left**). By comparison, WO-19 TILs displayed robust tumoricidal activity against autologous tumor cells (Fig. 4**, right;** average area under the curve (AUC), $p < 0.0001$). To determine whether blockade of the PD-1/PD-L1 axis enhanced TIL-mediated lysis, a PD-1 blocking antibody, pembrolizumab, was added to co-cultures. PD-1 blockade significantly increased the lytic activity of WO-19 TILs against autologous tumor cells (Fig. 4, **right**; AUC, $p < 0.0001$), but had no detectable impact on WO-12 TIL-mediated lysis (Fig. 4**, left**). Together, these results suggest that WO-19 TILs may possess augmented antitumor activity *in vivo*, compared to WO-12 TILs. Also, the activity of WO-19 TILs may be enhanced further through co-administration of anti-PD-1 therapy, while WO-12 TILs would be unaffected by PD-1 blockade when applied *in vivo*.

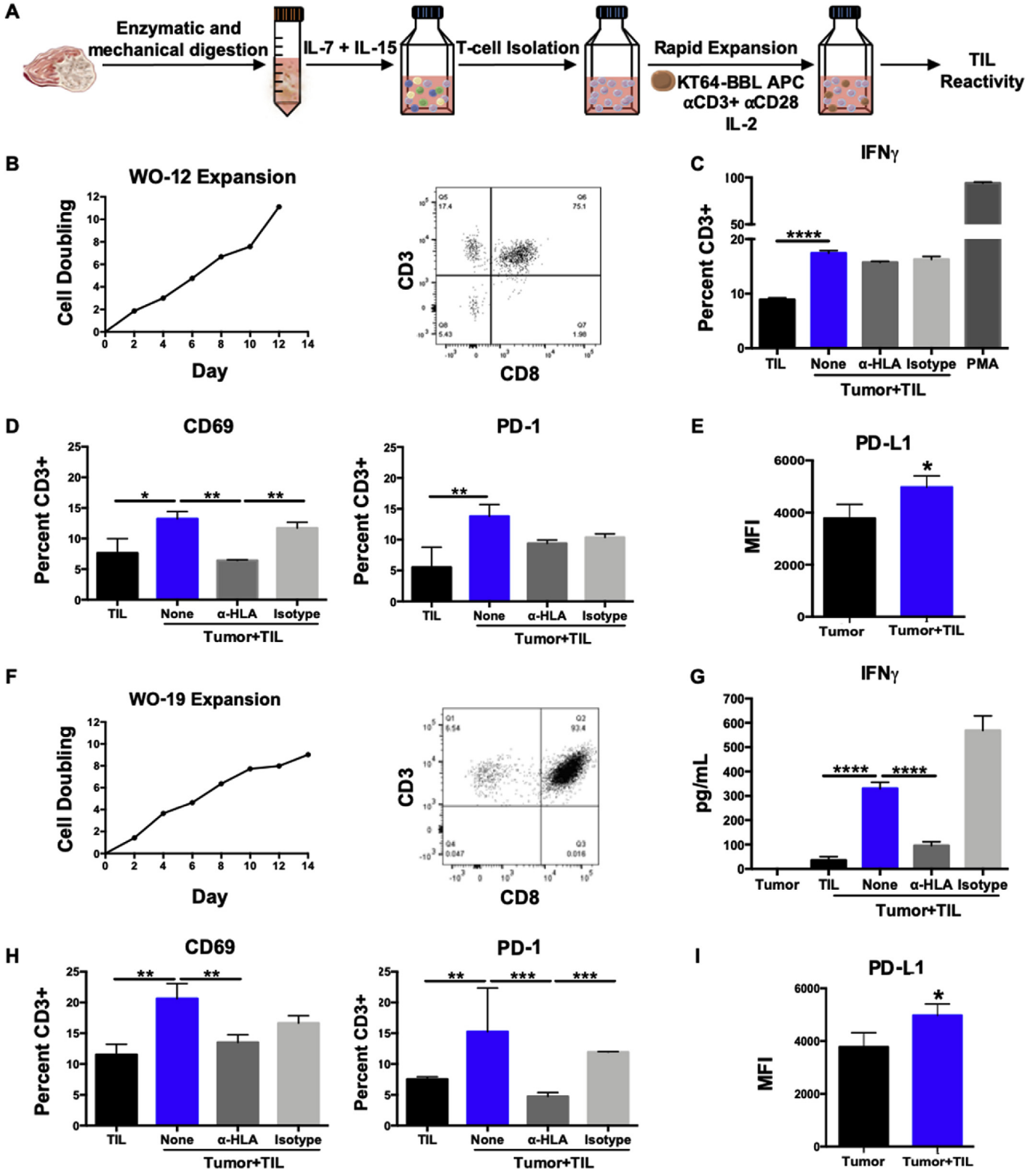

Fig. 3. Expanded autologous TILs co-cultured with patient-matched tumor cells. (A) Schematic of TIL digestion and expansion. Patient tumors are first enzymatically and mechanically digested. Tumor digests are incubated with IL-7 and IL-15 for 48 h prior to pan T-cell isolation. T-cells were isolated and then cultured with irradiated artificial antigen presenting cells (aAPCs) that were pre-coated with anti-CD3 and/or anti-CD28 (Day 0). Starting on day 2, cultures were supplemented with 600 IU/mL of IL-2 and maintained at a cell concentration of 0.6–1 x 10^6 cells/ml. After 12–14 days in culture, expanded T-cells were assessed for their reactivity. TIL doubling throughout rapid expansion protocol and scatter plots for $CD3^+CD8^+$ characterization at day 14 shown for primary patient samples WO-12 (B) and WO-19 (F). Autologous TILs were co-cultured with patient-matched WO-12 (C–E) of WO-19 (G–I) tumor cells with or without addition of α-HLA blocking peptide or isotype control for 24 h. (C) WO-12 T-cell specific IFNγ secretion was analyzed with a flow cytometry-based assay. $CD3^+IFN\gamma^+$ T-cells were gated first by forward side scatter then live dead staining. WO-12 (D) and WO-19 (H) T-cell activation marker CD69 and inhibitory marker PD-1 were analyzed via flow cytometry. Cells were first gated on forward side scatter for lymphocytes and then for live cells using a live dead fixable stain. Results are reported for percent of $CD45^+CD3^+$ T-cells expressing CD69 or PD-1. WO12 (E) and WO-19 (I) Tumor cell staining of T-cell inhibitory marker PD-L1 was analyzed via flow cytometry. Live tumor cells were gated first by forward side scatter then live dead staining. $CD45^-EPCAM^+PD\text{-}L1^+$ cells were analyzed for mean fluorescence intensity (MFI) of PD-L1. MFI of isotype control was subtracted from MFI of $CD45^-EPCAM^+PD\text{-}L1^+$ cells alone or co-cultured with TILs. (G) WO-19 co-culture supernatant was analyzed for IFNγ secretion by ELISA and reported as concentration (pg/mL). Data reported is a representative of three individual experiments and was analyzed by a one way-ANOVA and Tukey's multiple comparison pot-hoc test or unpaired T-test when appropriate. Mean ± SD (n = 3), *p < 0.05, **p < 0.01, ***p < 0.001, ****p < 0.0001.

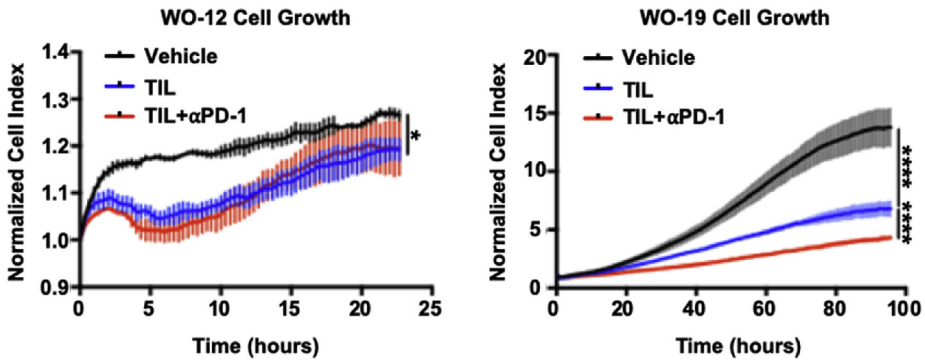

Fig. 4. Evaluation of cytotoxicity of TILs against autologous tumor cells with anti-PD-1. Dissociated WO-19 PDX tumor cells (4×10^4) or WO-12 primary tumor cells (1×10^4) were plated and allowed to adhere overnight. Cell growth was dynamically monitored using RT-CES system for 24–48 h. TILs were added at a 1:1 effector to target ratio and anti-PD-1 was added at a final concentration of 10 μg/mL. Current disruption measurements were automatically collected by the analyzer every 20 min over four days by xCELLigence technology. Significance was determined by one way-ANOVA comparison of the area under the curve, and is represented as mean ± SD (n = 3), *p < 0.05, ****p < 0.0001.

3.6. Autologous TILs in combination with anti-PD-1 in an orthotopic HGSOC PDX model

Clinically relevant HGSOC models that can be utilized to test the *in vivo* efficacy of immune therapies, such as checkpoint inhibitors, are lacking. With the co-development of well-characterized orthotopic HGSOC PDX models and patient-matched, tumor-reactive TIL cultures, we sought to develop a humanized PDX model with two goals. First, we sought to test the impact of the patient's immune system on tumor progression *in vivo*. Second, we aimed to enhance the endogenous immune reactivity through the application of immune checkpoint inhibition. NSG mice were orthotopically transplanted with MP3 tumors for pre-clinical studies (Fig. 5A). When PDX tumors reached ~70–100 mm^3, mice were randomized into TIL infusion alone, TIL infusion + anti PD-1, or vehicle control groups. Upon randomization, 1×10^7 autologous TILs were administered by intraperitoneal (i.p.) injection weekly. Following TIL injections, mice received 10 mg/kg anti PD-l by i.p. injection, twice per week. This dosing strategy was repeated over a 6 week course, or until the mouse was euthanized due to tumor volume exceeding 1000 mm^3.

In the WO-12 PDX model, administration of TILs significantly reduced tumor volume at 6 weeks (Fig. 5B, 2-way ANOVA, $p = 0.0098$), but did not significantly impact survival compared to the vehicle control group (Log-rank, $p = 0.3430$). The median survival of untreated mice was 8 weeks, compared to a median survival of 18 weeks for mice that received TIL transfer, however due to small sample size these effects did not reach significance (Log rank test, $p = 0.2122$). In this model, the addition of anti-PD-1 antibody had no significant additive effects on $CD3^+$ T-cell infiltration, tumor volume or survival (Fig. 5B and S3A), mimicking the results of co-culture assays (Fig. 4).

In comparison, the studies utilizing the WO-19 TIL/PDX model did result in significant effects when anti-PD-1 therapy was administered. At four weeks post-treatment, groups receiving autologous TILs alone had modestly reduced tumor volumes compared to vehicle control mice (AUC, $p = 0.5349$; 2-way ANOVA, $p = 0.0053$). Mice administered both TIL and anti-PD-1 has significantly reduced average tumor volume compared to untreated WO-19 mice (AUC, $p = 0.0202$; 2-way ANOVA $p < 0.0001$, Figs. 5C and S3B). TILs and anti-PD-1 significantly reduced tumor volume compared to TILs alone at five and six weeks post-randomization (2-way ANOVA, $p = 0.0317$ and $p = 0.0002$, respectfully). TIL infusion alone did not increase overall survival compared to untreated mice, however, TIL infusion plus anti-PD-1 therapy increased overall survival (Log rank test $p = 0.0057$) compared to both the TILs alone and the vehicle control groups ($p = 0.0084$ and $p = 0.0069$, respectfully). For mice humanized with TILs, the addition of anti-PD-1 therapy increased the median survival from 5 to 7 weeks, compared to untreated mice (ANOVA, $p = 0.0022$, Fig. 5C). Five weeks post-randomization, all of the mice in the untreated groups had tumors with volumes >1000mm3 and were euthanized, whereas all mice who received autologous TILs plus anti-PD-1 had lower tumor burden (Fig. 5C).

The primary goal of checkpoint inhibitor treatment is to bolster endogenous anti-tumor T-cell activity. Upon euthanasia, tumors were collected and IHC was performed in order to assess relative intraepithelial $CD3^+$ T-cell accumulation amongst the various treatment groups. Representative images of $CD3^+$ staining are shown (Fig. 5D). Although the overall number of infiltrating T-cells was not significantly different between treatments groups, there was a trend toward an increase in the average number of intraepithelial T-cells in the TIL plus anti-PD-1 group (Fishes Least Squared Difference Test $p = 0.0390$), which correlated to overall survival and tumor burden.

Clear cell carcinomas are generally less responsive to chemotherapy [35,36], but may have increased sensitivity to immunotherapy [37]. We therefore utilized an established PDX model derived from a mixed HGSOC with clear cell to test the activity of anti-PD-1 antibody therapy. Prior to *in vivo* studies, we tested tumor reactivity in *ex vivo* co-cultures and found that similar to WO-19, IFNγ secretion and CD69 surface expression is upregulated in an HLA 1 dependent manner. MHC II neutralizing peptides did not further reduce the level of CD3 activation, suggesting that $CD8^+$ T-cells, not $CD4^+$ T cells, are the major mediators of the response to autologous tumor cells in this model (Fig. S4C).

To determine if anti-PD-1 therapy was efficacious at reducing tumor burden in the WO-6 TIL/PDX model, an endpoint *in vivo* study was performed. Since the WO-6 PDX model showed increased baseline growth kinetics, tumors were orthotopically transplanted, and then mice were randomized and administered with 1×10^7 autologous TILs four days later (Fig. S4D). One and 4 days following each TIL administration, mice received 10 mg/kg anti PD-l or IgG4 kappa isotype by i.p. administration. Most untreated mice required euthanization due to tumor progression (>1000 mm^3 tumor volume) by 20 days. Upon euthanization at day 20, $CD3^+$ and $CD3^+CD8^+$ peripheral T cells were quantified by flow cytometry. The addition of IgG4 to TIL administration did not significantly increase the number of peripheral $CD3^+$ or $CD3^+CD8^+$ T cells compared to the TILs alone arm. However, administration of anti-PD-1 antibody did significantly increase the quantity of circulating T-cells compared to TILs alone ($CD3^+$, $p = 0.0289$; $CD3^+CD8$, $p = 0.0258$, Fig. S4E). Mice treated with TILs and anti-PD-1 showed a significant reduction in tumor burden, compared to TILs

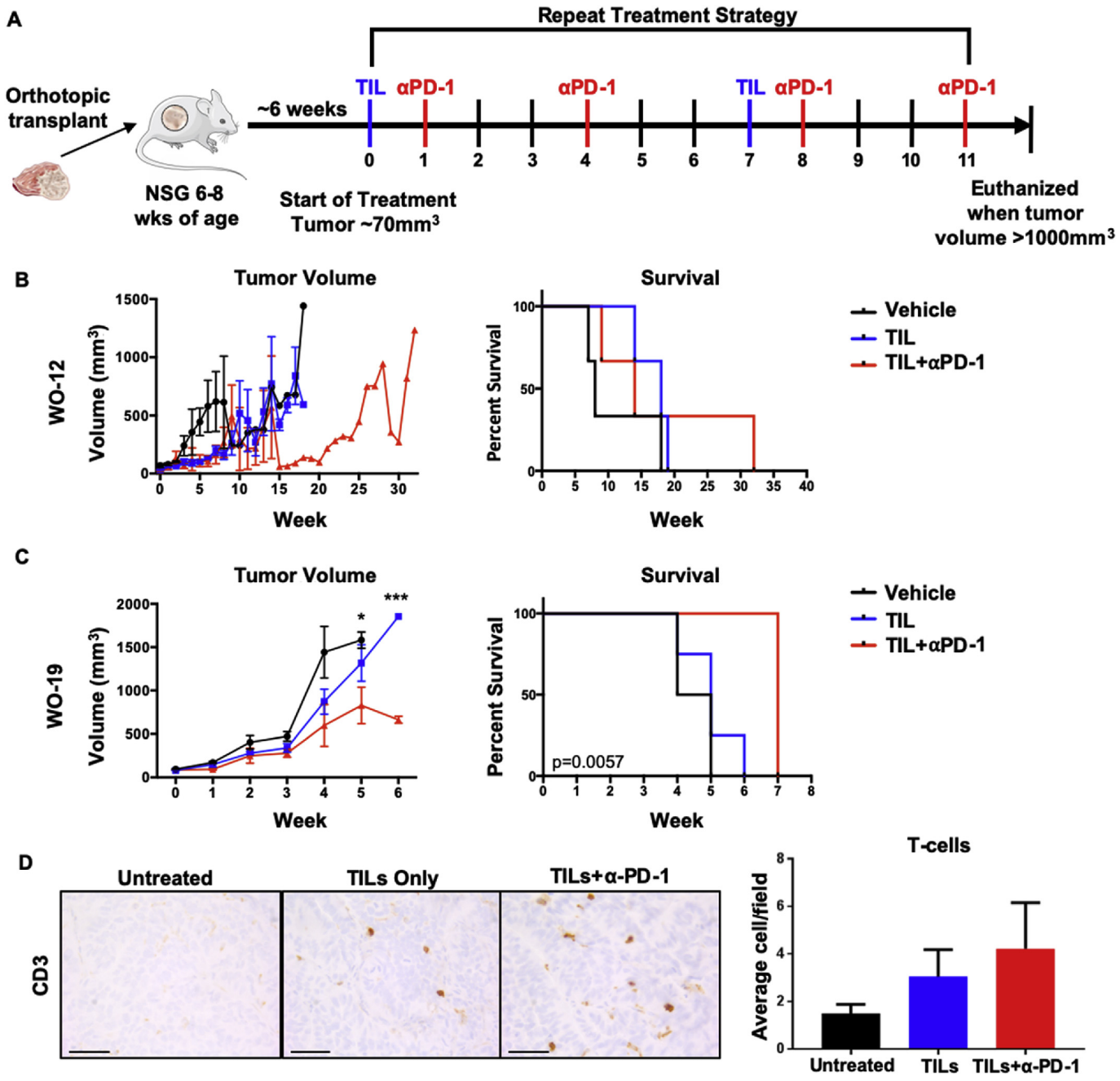

Fig. 5. Autologous TILs in combination with anti-PD-1 in an orthotopic PDX model for HGSOC. (A) Schematic of *in vivo* patient-matched autologous PDX pre-clinical studies. Orthotopically transplanted NSG mice were randomized to various arms when the tumor volume reached approximately 70 mm^3. Treated mice were dosed with a weekly regime of 1×10^7 TILs following 2 doses of 10 mg/kg α-PD-1 or PBS as a control. The dosing strategy was repeated for up to 6 weeks or until the mouse was euthanized with a tumor volume $\geq$1000 m^3. WO-12 (B, left) and WO-19 (C, left) tumor volume was measured via ultrasound weekly. Data is represented as mean ± SEM. Data was analyzed by two way-ANOVA, and significance is shown for TIL vs TIL + anti-PD-1 comparisons, $^*p < 0.05$, $^{***}p < 0.001$. (B, right) Kaplan Meier curve for WO-12 survival study shows that TIL therapy alone or in combination with anti-PD-1 did not significantly increase survival (n = 3 per group, Log-rank Mantel-Cox test, p = 0.3520). (C, right) Survival curve for WO-19 PDX tumors exhibit longer survival when treated with autologous TIL therapy in combination with α-PD-1. Kaplan Meier curves for survival (n ≈ 5 for each group) show that TIL therapy alone did not significantly increase survival. Survival was significantly increased for mice with combination treatment of TIL + α-PD-1 compared to untreated mice (Log-rank Mantel-Cox test, p = 0.0069). (D) At euthanization, PDX tumors from donor WO-19 was harvested and stained for human CD3. (D, right) Intratumor $CD3^+$ T-cells was quantified, and data is represented as the mean ± SD of $CD3^+$ T-cells from 40 to 60 10x fields.

with IgG4 isotype control (ANOVA, p = 0.003, Fig. S4F). There was a trend for an increased number of intraepithelial T-cells ($CD3^+$) in all groups that were administered TILs, however this only reached statistical significance for the group treated with TILs alone (ANOVA, p = 0.0457, Fig. S4G). In summary, we demonstrate that the autologous patient-matched TIL/PDX model is a unique platform to assess patient-specific T-cell response to immunotherapy.

4. Discussion

Advanced stage HGSOC often recurs and cure is relatively rare [38]. Immunotherapies have significantly improved patient outcome in several non-gynecological cancers such as melanoma, lung, renal and colon cancer leading to FDA approval [18–20]. However, immunotherapies to date have demonstrated only

modest clinical responses for HGSOC [20,21]. Immunomodulatory agents as monotherapies will likely be inadequate in the recurrent setting for this disease [20,23]. To date, we have not optimized *when* (e.g. upfront treatment, maintenance setting, or at time of recurrence) and *how* (e.g. in combination with cytotoxic drugs or with other immunotherapies, or by concomitant vs sequencing schedules) immunotherapies should be utilized in HGSOC. Preclinical model systems that mimic the biology of the original patient tumor and incorporate the patient's immune system are critical to understand, and optimize immunotherapies to ultimately guide human clinical trial design.

There are a lack of preclinical *in vivo* models that both accurately recapitulate human HGSOC and enable the testing of immune modulating therapies that effect adaptive immune responses. Current model systems generally utilize immunocompetent syngeneic and genetically engineered mice, or immune-deficient HGSOC xenograft mouse models. Of these models, only xenograft models bear human tumors, and since these models generally lack a functional immune system, they are ineffective for testing immunotherapies. To overcome this challenge, three general models have been previously developed which have a limited immune component reconstituted *in vivo* [29]. First, models have been humanized by inoculating healthy human PBMCs from donors, which contain mature human T-cells. Donor PBMCs are readily available and cost effective, but are often immunologically mismatched to the tumor and rarely possess autologous anti-tumor activity. Second, models have been humanized by inoculating human CD34 $^{+}$ cells, stem cells derived from the bone marrow, umbilical cord, or fetal thymus. In this case, all human hematopoietic lineages are represented, but not all are functionally developed. T-cells developing in this system seldom experience central tolerance induction, have not been previously exposed to the hostile tumor microenvironment, and are seldom matched to the engrafted tumor. Also, erroneously trained T-cells and other cells from the hematopoietic system frequently cause graft-vs-host disease [28]. Although these preclinical models can be informative, they lack a tumor-primed, autologous immune component that may better predict patient-specific responses in a heterogeneous disease such as HGSOC.

Here we developed a two-tiered platform for testing the efficacy of novel immunomodulating therapeutics or combinations, in autologous patient-matched TIL/PDX models. First, TIL reactivity was tested *ex vivo* in order to provide an indication of the predictive response to therapeutics *in vivo*. Expanded TILs were activated when co-cultured with patient-matched tumor cells *in vitro*, signified by an HLA-dependent increase in IFNγ production and expression of cell surface activation markers CD69 and PD-1. Moreover, tumor-specific expression of PD-L1 was induced in the presence of autologous TILs. Due to the increased expression of PD-1 on T-cells and concomitant PD-L1 on tumor cells, studies were conducted to determine if disruption of the PD-1/PD-L1 axis would increase tumor reactivity of the expanded TILs. Anti-PD-1 was added to TIL and tumor co-cultures and tumor lysis was analyzed. These studies demonstrated that the addition of anti-PD-1 therapy in one model (WO-19) increased tumor lysis *ex vivo,* which rationalized the testing of anti-PD-1 therapy *in vivo*.

The second tier of the platform utilized a novel orthotopic HGSOC PDX model transferred with patient-matched tumor-reactive TILs to test the efficacy of anti-PD-1 checkpoint inhibitor therapy. These PDX models maintain the genetic characteristics of the primary patient tumor however much of the immune cell components do not persist after serial passaging. Immunohistochemical profiling of the T-cells indicated that some human CD3 T-cells are maintained in the WO-19 PDX tumors however almost all human CD8^{+} T-cells are diminished. We find that reintroduction of CD8^{+} TILs controlled HGSOC progression *in vivo*, which could be enhanced by the addition of immune checkpoint blockade therapy (Fig. 5 and S4).

Anti-PD-1 therapy was tested in the three distinct and newly developed autologous TIL/PDX models of HGSOC. In the WO-12 model, the addition of anti-PD-1 did not increase survival in mice. These results were not surprising since *ex vivo* co-culture results indicated reduced CD8^{+} TIL activity (Fig. 3) and a minimal impact from the addition of anti-PD-1 to the tumor lysis assay (Fig. 4). Moreover, the WO-12 PDX model displayed lower overall PD-1 staining and fewer CD4 T-cells retained from the original patient tumor (Fig. 2) when compared to the WO-19 model. However, in the WO-19 (*CCNE1* amplified) model, TIL infusion plus anti-PD-1 reduced overall tumor burden, and significantly increased survival compared to TIL alone and vehicle treated mice. Compared to WO-12, PDX models from this donor had higher PD-1 expression in regions with residual CD4^{+} T-cells, which could have an added effect when treated with anti-PD-1. In a highly aggressive WO-6 model of *BRCA1*^{mut} HGSOC with clear cell changes, tumor burden was significantly reduced when TILs and anti-PD-1 were administered, compared to when TILs were administered with the IgG control. This finding is of particular interest since many clear cell ovarian carcinomas are characterized by an immunosuppressive microenvironment [39], high microsatellite instability or mismatch repair deficiency, increased neoantigen burden [40], and PD-L1 expression by tumors [41.] and the expression of PD-1 on TILs and PD-L1 on tumor cells is reported to correlate with clinical outcome [42,43]. More so, patients with clear cell ovarian carcinomas may be more sensitive to immune checkpoint blockade therapy using PD-1 and PD-L1 inhibitors [22,44,45] than other ovarian cancer histologies. As such, the WO-6 model TIL/PDX model provides a unique opportunity to identify and enhance the mechanisms controlling responsiveness to immunotherapy in this subset of ovarian cancer patients.

In the examination of tumors resected at the end of study, treatment with TILs did not appear to induce sustained PD-L1 expression in the tumor microenvironment in the TIL/PDX models (data not shown). It remains possible that, in the early aftermath of TIL infusion, locally secreted IFNγ by transferred TILs results in transient increases in tumor PD-L1 expression, thereby creating a PD-1/PD-L1 axis of immune suppression which was overcome by the administration of anti-PD-1 therapy. Deeper longitudinal studies will aid in understanding the underpinnings of anti-PD-1 therapies in this model, however, it may be expected that greater efficacy may be achieved in additional TIL/PDX models that have higher baseline endogenous PD-L1 expression *in vivo*.

Our new humanized TIL/PDX platform has been shown to have preclinical applications when testing immunotherapies *in vitro* and *in vivo*. Unlike other preclinical models, our humanized TIL/PDX models utilize patient-matched TILs to evaluate the anti-tumor effect of immunomodulating therapies against autologous-tumors. As these TILs have already been primed to the heterogeneity of the autologous tumor, *ex vivo* engineering of the T-cell receptor repertoire is unnecessary. However, there are still some inherent limitations to the current model, for example, a lack of innate immune cells (i.e. tumor associated macrophages), and the known chimeric nature of the tumor vasculature. Furthermore, the development of each model remains reliant on the availability of patient tumor material and successful TIL expansion. Yet, the autologous nature of this system is designed to limit allogeneic immune responses against cancer and to serve as a platform for the testing of highly personalized, patient-specific responses to immune interventions.

Acknowledgements

This work was supported by the Penn Ovarian Cancer Translational Center of Excellence at the Abramson Cancer Center,

Ovarian Cancer Research Center (awarded to F.S. and D.J.P.), Ovarian Cancer Research Alliance and Rivkin Center for Ovarian Cancer (awarded to S.B.G.). Additionally, we would like to thank the Penn Stem Cell and Xenograft Core for providing mice for animal studies, and finally University of Pennsylvania and Harvard University Histology cores.

Appendix A. Supplementary data

Supplementary data to this article can be found online at https://doi.org/10.1016/j.ygyno.2019.10.011.

Declaration of competing InterestCOI

The authors declare no potential conflicts of interest.

Author contribution

S.B.G., H.K., S.R., A.G.R. participated in experimental design, conducted experiments, collected, analyzed and interpreted data. D.O. processed primary tumor samples, performed *in vitro* cell expansion, and performed blood analysis. S.M., Y.K. assisted with *in vivo* studies. A.J.F assisted with immunohistochemistry. H.X. established and provided primary tumor cultures. L.E.S. compiled and analyzed data. D.J.P. participated in experimental design, contributed to data analysis and interpretation. F.S. provided primary patient samples, developed the orthotopic transplant PDX models, participated in experimental design, contributed to data analysis and interpretation. S.B.G. wrote the manuscript. All authors assisted in writing and editing the manuscript.

References

[1] American Cancer Society, Cancer Facts & Figures 2019, American Cancer Society, Atlanta, Ga, 2019.
[2] M.K. Parmar, J.A. Ledermann, N. Colombo, A. du Bois, J.F. Delaloye, G.B. Kristensen, S. Wheeler, A.M. Swart, W. Qian, V. Torri, I. Floriani, G. Jayson, A. Lamont, C. Trope, Collaborators AGO. Icon, Paclitaxel plus platinum-based chemotherapy versus conventional platinum-based chemotherapy in women with relapsed ovarian cancer: the ICON4/AGO-OVAR-2.2 trial, Lancet 361 (9375) (2003) 2099–2106. PubMed PMID: 12826431.
[3] M. Binju, M.A. Padilla, T. Singomat, P. Kaur, Y. Suryo Rahmanto, P.A. Cohen, Y. Yu, Mechanisms underlying acquired platinum resistance in high grade serous ovarian cancer - a mini review, Biochim. Biophys. Acta Gen. Subj. 1863 (2) (2019) 371–378, https://doi.org/10.1016/j.bbagen.2018.11.005. PubMed PMID: 30423357.
[4] Cancer Genome Atlas Research N, Integrated genomic analyses of ovarian carcinoma, Nature 474 (7353) (2011) 609–615, https://doi.org/10.1038/nature10166. PubMed PMID: 21720365; PMCID: PMC3163504.
[5] B. Kaufman, R. Shapira-Frommer, R.K. Schmutzler, M.W. Audeh, M. Friedlander, J. Balmana, G. Mitchell, G. Fried, S.M. Stemmer, A. Hubert, O. Rosengarten, M. Steiner, N. Loman, K. Bowen, A. Fielding, S.M. Domchek, Olaparib monotherapy in patients with advanced cancer and a germline BRCA1/2 mutation, J. Clin. Oncol. 33 (3) (2015) 244–250, https://doi.org/10.1200/JCO.2014.56.2728. PubMed PMID: 25366685; PMCID: PMC6057749.
[6] E.M. Swisher, K.K. Lin, A.M. Oza, C.L. Scott, H. Giordano, J. Sun, G.E. Konecny, R.L. Coleman, A.V. Tinker, D.M. O'Malley, R.S. Kristeleit, L. Ma, K.M. Bell-McGuinn, J.D. Brenton, J.M. Cragun, A. Oaknin, I. Ray-Coquard, M.I. Harrell, E. Mann, S.H. Kaufmann, A. Floquet, A. Leary, T.C. Harding, S. Goble, L. Maloney, J. Isaacson, A.R. Allen, L. Rolfe, R. Yelensky, M. Raponi, I.A. McNeish, Rucaparib in relapsed, platinum-sensitive high-grade ovarian carcinoma (ARIEL2 Part 1): an international, multicentre, open-label, phase 2 trial, Lancet Oncol. 18 (1) (2017) 75–87, https://doi.org/10.1016/S1470-2045(16)30559-9. PubMed PMID: 27908594.
[7] R.D. Morgan, A.R. Clamp, D.G.R. Evans, R.J. Edmondson, G.C. Jayson, PARP inhibitors in platinum-sensitive high-grade serous ovarian cancer, Cancer Chemother. Pharmacol. 81 (4) (2018) 647–658, https://doi.org/10.1007/s00280-018-3532-9. PubMed PMID: 29464354; PMCID: PMC5854713.
[8] A.M. Karst, P.M. Jones, N. Vena, A.H. Ligon, J.F. Liu, M.S. Hirsch, D. Etemadmoghadam, D.D. Bowtell, R. Drapkin, Cyclin E1 deregulation occurs early in secretory cell transformation to promote formation of fallopian tube-derived high-grade serous ovarian cancers, Cancer Res. 74 (4) (2014) 1141–1152, https://doi.org/10.1158/0008-5472.CAN-13-2247. PubMed PMID: 24366882; PMCID: PMC4517944.
[9] A.M. Patch, E.L. Christie, D. Etemadmoghadam, D.W. Garsed, J. George, S. Fereday, K. Nones, P. Cowin, K. Alsop, P.J. Bailey, K.S. Kassahn, F. Newell, M.C. Quinn, S. Kazakoff, K. Quek, C. Wilhelm Benartzi, E. Curry, H.S. Leong, Australian Ovarian Cancer Study G, A. Hamilton, L. Mileshkin, G. Au-Yeung, C. Kennedy, J. Hung, Y.E. Chiew, P. Harnett, M. Friedlander, M. Quinn, J. Pyman, S. Cordner, P. O'Brien, J. Leditschke, G. Young, K. Strachan, P. Waring, W. Azar, C. Mitchell, N. Traficante, J. Hendley, H. Thorne, M. Shackleton, D.K. Miller, G.M. Arnau, R.W. Tothill, T.P. Holloway, T. Semple, I. Harliwong, C. Nourse, E. Nourbakhsh, S. Manning, S. Idrisoglu, T.J. Bruxner, A.N. Christ, B. Poudel, O. Holmes, M. Anderson, C. Leonard, A. Lonie, N. Hall, S. Wood, D.F. Taylor, Q. Xu, J.L. Fink, N. Waddell, R. Drapkin, E. Stronach, H. Gabra, R. Brown, A. Jewell, S.H. Nagaraj, E. Markham, P.J. Wilson, J. Ellul, O. McNally, M.A. Doyle, R. Vedururu, C. Stewart, E. Lengyel, J.V. Pearson, N. Waddell, A. deFazio, S.M. Grimmond, D.D. Bowtell, Whole-genome characterization of chemoresistant ovarian cancer, Nature 521 (7553) (2015) 489–494, https://doi.org/10.1038/nature14410. PubMed PMID: 26017449.
[10] D. Etemadmoghadam, A. deFazio, R. Beroukhim, C. Mermel, J. George, G. Getz, R. Tothill, A. Okamoto, M.B. Raeder, P. Harnett, S. Lade, L.A. Akslen, A.V. Tinker, B. Locandro, K. Alsop, Y.E. Chiew, N. Traficante, S. Fereday, D. Johnson, S. Fox, W. Sellers, M. Urashima, H.B. Salvesen, M. Meyerson, D. Bowtell, A.S. Group, Integrated genome-wide DNA copy number and expression analysis identifies distinct mechanisms of primary chemoresistance in ovarian carcinomas, Clin. Cancer Res. 15 (4) (2009) 1417–1427, https://doi.org/10.1158/1078-0432.CCR-08-1564. PubMed PMID: 19193619; PMCID: PMC2670486.
[11] D. Aziz, D. Etemadmoghadam, C.E. Caldon, G. Au-Yeung, N. Deng, R. Hutchinson, Australian Ovarian Cancer Study G, Bowtell D, Waring P. 19q12 amplified and non-amplified subsets of high grade serous ovarian cancer with overexpression of cyclin E1 differ in their molecular drivers and clinical outcomes, Gynecol. Oncol. 151 (2) (2018) 327–336, https://doi.org/10.1016/j.ygyno.2018.08.039. PubMed PMID: 30209015.
[12] L. Zhang, J.R. Conejo-Garcia, D. Katsaros, P.A. Gimotty, M. Massobrio, G. Regnani, A. Makrigiannakis, H. Gray, K. Schlienger, M.N. Liebman, S.C. Rubin, G. Coukos, Intratumoral T cells, recurrence, and survival in epithelial ovarian cancer, N. Engl. J. Med. 348 (3) (2003) 203–213, https://doi.org/10.1056/NEJMoa020177. PubMed PMID: 12529460.
[13] Q. Ye, D.G. Song, M. Poussin, T. Yamamoto, A. Best, C. Li, G. Coukos, D.J. Powell Jr., CD137 accurately identifies and enriches for naturally occurring tumor-reactive T cells in tumor, Clin. Cancer Res. 20 (1) (2014) 44–55, https://doi.org/10.1158/1078-0432.CCR-13-0945. PubMed PMID: 24045181; PMCID: PMC3947326.
[14] J.R. Webb, K. Milne, D.R. Kroeger, B.H. Nelson, PD-L1 expression is associated with tumor-infiltrating T cells and favorable prognosis in high-grade serous ovarian cancer, Gynecol. Oncol. 141 (2) (2016) 293–302, https://doi.org/10.1016/j.ygyno.2016.03.008. PubMed PMID: 26972336.
[15] K. Abiko, N. Matsumura, J. Hamanishi, N. Horikawa, R. Murakami, K. Yamaguchi, Y. Yoshioka, T. Baba, I. Konishi, M. Mandai, IFN-gamma from lymphocytes induces PD-L1 expression and promotes progression of ovarian cancer, Br. J. Canc. 112 (9) (2015) 1501–1509, https://doi.org/10.1038/bjc.2015.101. PubMed PMID: 25867264; PMCID: PMC4453666.
[16] L.M. Francisco, V.H. Salinas, K.E. Brown, V.K. Vanguri, G.J. Freeman, V.K. Kuchroo, A.H. Sharpe, PD-L1 regulates the development, maintenance, and function of induced regulatory T cells, J. Exp. Med. 206 (13) (2009) 3015–3029, https://doi.org/10.1084/jem.20090847. PubMed PMID: 20008522; PMCID: PMC2806460.
[17] V.R. Juneja, K.A. McGuire, R.T. Manguso, M.W. LaFleur, N. Collins, W.N. Haining, G.J. Freeman, A.H. Sharpe, PD-L1 on tumor cells is sufficient for immune evasion in immunogenic tumors and inhibits CD8 T cell cytotoxicity, J. Exp. Med. 214 (4) (2017) 895–904, https://doi.org/10.1084/jem.20160801. PubMed PMID: 28302645; PMCID: PMC5379970.
[18] J. Gong, A. Chehrazi-Raffle, S. Reddi, R. Salgia, Development of PD-1 and PD-L1 inhibitors as a form of cancer immunotherapy: a comprehensive review of registration trials and future considerations, J Immunother Cancer 6 (1) (2018) 8, https://doi.org/10.1186/s40425-018-0316-z. PubMed PMID: 29357948; PMCID: PMC5778665.
[19] L. Chen, X. Han, Anti-PD-1/PD-L1 therapy of human cancer: past, present, and future, J. Clin. Investig. 125 (9) (2015) 3384–3391, https://doi.org/10.1172/JCI80011. PubMed PMID: 26325035; PMCID: PMC4588282.
[20] J. Hamanishi, M. Mandai, N. Matsumura, K. Abiko, T. Baba, I. Konishi, PD-1/PD-L1 blockade in cancer treatment: perspectives and issues, Int. J. Clin. Oncol. 21 (3) (2016) 462–473, https://doi.org/10.1007/s10147-016-0959-z. PubMed PMID: 26899259; PMCID: PMC4901122.
[21] J. Hamanishi, M. Mandai, T. Ikeda, M. Minami, A. Kawaguchi, T. Murayama, M. Kanai, Y. Mori, S. Matsumoto, S. Chikuma, N. Matsumura, K. Abiko, T. Baba, K. Yamaguchi, A. Ueda, Y. Hosoe, S. Morita, M. Yokode, A. Shimizu, T. Honjo, I. Konishi, Safety and antitumor activity of anti-PD-1 antibody, nivolumab, in patients with platinum-resistant ovarian cancer, J. Clin. Oncol. 33 (34) (2015) 4015–4022, https://doi.org/10.1200/JCO.2015.62.3397. PubMed PMID: 26351349.
[22] U.A. Matulonis, R. Shapira-Frommer, A.D. Santin, A.S. Lisyanskaya, S. Pignata, I. Vergote, F. Raspagliesi, G.S. Sonke, M. Birrer, D.M. Provencher, J. Sehouli, N. Colombo, A. Gonzalez-Martin, A. Oaknin, P.B. Ottevanger, V. Rudaitis, K. Katchar, H. Wu, S. Keefe, J. Ruman, J.A. Ledermann, Antitumor activity and safety of pembrolizumab in patients with advanced recurrent ovarian cancer: results from the phase II KEYNOTE-100 study, Epub 2019/05/03, Ann. Oncol. 30 (7) (2019) 1080–1087, https://doi.org/10.1093/annonc/mdz135. PubMed PMID: 31046082.
[23] R. Burger, M. Sill, D. Zamarin, D. Powell, I. Frak, O. Zivanovic, C. Gunderson, E. Ko, C. Matthews, S. Sharma, A. Hagemann, S. Khleif, C. Aghajanian, NRG

oncology phase II randomized trial of nivolumab with or without ipilimuab in patients with persistant or recurrent ovarian cancer, J. Clin. Oncol. 33 (15_suppl) (2018).

[24] E. George, H. Kim, C. Krepler, B. Wenz, M. Makvandi, J.L. Tanyi, E. Brown, R. Zhang, P. Brafford, S. Jean, R.H. Mach, Y. Lu, G.B. Mills, M. Herlyn, M. Morgan, X. Zhang, R. Soslow, R. Drapkin, N. Johnson, Y. Zheng, G. Cotsarelis, K.L. Nathanson, F. Simpkins, A patient-derived-xenograft platform to study BRCA-deficient ovarian cancers, JCI Insight 2 (1) (2017), e89760, https://doi.org/10.1172/jci.insight.89760. PubMed PMID: 28097235; PMCID: PMC5214535.

[25] Y. Lai, X. Wei, S. Lin, L. Qin, L. Cheng, P. Li, Current status and perspectives of patient-derived xenograft models in cancer research, J. Hematol. Oncol. 10 (1) (2017) 106, https://doi.org/10.1186/s13045-017-0470-7. PubMed PMID: 28499452; PMCID: PMC5427553.

[26] J.F. Liu, S. Palakurthi, Q. Zeng, S. Zhou, E. Ivanova, W. Huang, I.K. Zervantonakis, L.M. Selfors, Y. Shen, C.C. Pritchard, M. Zheng, V. Adleff, E. Papp, H. Piao, M. Novak, S. Fotheringham, G.M. Wulf, J. English, P.T. Kirschmeier, V.E. Velculescu, C. Paweletz, G.B. Mills, D.M. Livingston, J.S. Brugge, U.A. Matulonis, R. Drapkin, Establishment of patient-derived tumor xenograft models of epithelial ovarian cancer for preclinical evaluation of novel therapeutics, Clin. Cancer Res. 23 (5) (2017) 1263–1273, https://doi.org/10.1158/1078-0432.CCR-16-1237. PubMed PMID: 27573169; PMCID: PMC5332350.

[27] T.K. Owonikoko, G. Zhang, H.S. Kim, R.M. Stinson, R. Bechara, C. Zhang, Z. Chen, N.F. Saba, S. Pakkala, R. Pillai, X. Deng, S.Y. Sun, M.R. Rossi, G.L. Sica, S.S. Ramalingam, F.R. Khuri, Patient-derived xenografts faithfully replicated clinical outcome in a phase II co-clinical trial of arsenic trioxide in relapsed small cell lung cancer, J. Transl. Med. 14 (1) (2016) 111, https://doi.org/10.1186/s12967-016-0861-5. PubMed PMID: 27142472; PMCID: PMC4855771.

[28] H.R. Kim, H.N. Kang, H.S. Shim, E.Y. Kim, J. Kim, D.J. Kim, J.G. Lee, C.Y. Lee, M.H. Hong, S.M. Kim, H. Kim, K.H. Pyo, M.R. Yun, H.J. Park, J.Y. Han, H.A. Youn, M.J. Ahn, S. Paik, T.M. Kim, B.C. Cho, Co-clinical trials demonstrate predictive biomarkers for dovitinib, an FGFR inhibitor, in lung squamous cell carcinoma, Ann. Oncol. 28 (6) (2017) 1250–1259, https://doi.org/10.1093/annonc/mdx098. PubMed PMID: 28460066.

[29] P. De La Rochere, S. Guil-Luna, D. Decaudin, G. Azar, S.S. Sidhu, E. Piaggio, Humanized mice for the study of immuno-oncology, Trends Immunol. 39 (9) (2018) 748–763, https://doi.org/10.1016/j.it.2018.07.001. PubMed PMID: 30077656.

[30] T.A. Ince, A.D. Sousa, M.A. Jones, J.C. Harrell, E.S. Agoston, M. Krohn, L.M. Selfors, W. Liu, K. Chen, M. Yong, P. Buchwald, B. Wang, K.S. Hale, E. Cohick, P. Sergent, A. Witt, Z. Kozhekbaeva, S. Gao, A.T. Agoston, M.A. Merritt, R. Foster, B.R. Rueda, C.P. Crum, J.S. Brugge, G.B. Mills, Characterization of twenty-five ovarian tumour cell lines that phenocopy primary tumours, Nat. Commun. 6 (2015) 7419, https://doi.org/10.1038/ncomms8419. PubMed PMID: 26080861; PMCID: PMC4473807.

[31] Q. Ye, M. Loisiou, B.L. Levine, M.M. Suhoski, J.L. Riley, C.H. June, G. Coukos, D.J. Powell Jr., Engineered artificial antigen presenting cells facilitate direct and efficient expansion of tumor infiltrating lymphocytes, J. Transl. Med. 9 (2011) 131, https://doi.org/10.1186/1479-5876-9-131. PubMed PMID: 21827675; PMCID: PMC3162913.

[32] J.W. Cassidy, C. Caldas, A. Bruna, Maintaining tumor heterogeneity in patient-derived tumor xenografts, Cancer Res. 75 (15) (2015) 2963–2968, https://doi.org/10.1158/0008-5472.CAN-15-0727. PubMed PMID: 26180079; PMCID: PMC4539570.

[33] E. Lengyel, J.E. Burdette, H.A. Kenny, D. Matei, J. Pilrose, P. Haluska, K.P. Nephew, D.B. Hales, M.S. Stack, Epithelial ovarian cancer experimental models, Oncogene 33 (28) (2014) 3619–3633, https://doi.org/10.1038/onc.2013.321. PubMed PMID: 23934194; PMCID: PMC3990646.

[34] N. Nakayama, K. Nakayama, Y. Shamima, M. Ishikawa, A. Katagiri, K. Iida, K. Miyazaki, Gene amplification CCNE1 is related to poor survival and potential therapeutic target in ovarian cancer, Cancer 116 (11) (2010) 2621–2634, https://doi.org/10.1002/cncr.24987. PubMed PMID: 20336784.

[35] T. Sugiyama, A. Okamoto, T. Enomoto, T. Hamano, E. Aotani, Y. Terao, N. Suzuki, M. Mikami, N. Yaegashi, K. Kato, H. Yoshikawa, Y. Yokoyama, H. Tanabe, K. Nishino, H. Nomura, J.W. Kim, B.G. Kim, S. Pignata, J. Alexandre, J. Green, S. Isonishi, F. Terauchi, K. Fujiwara, D. Aoki, Randomized phase III trial of irinotecan plus cisplatin compared with paclitaxel plus carboplatin as first-line chemotherapy for ovarian clear cell carcinoma: JGOG3017/GCIG trial, Epub 2016/07/13, J. Clin. Oncol. 34 (24) (2016) 2881–2887, https://doi.org/10.1200/JCO.2016.66.9010. PubMed PMID: 27400948.

[36] T. Sugiyama, T. Kamura, J. Kigawa, N. Terakawa, Y. Kikuchi, T. Kita, M. Suzuki, I. Sato, K. Taguchi, Clinical characteristics of clear cell carcinoma of the ovary: a distinct histologic type with poor prognosis and resistance to platinum-based chemotherapy, Cancer 88 (11) (2000) 2584–2589. Epub 2000/06/22. PubMed PMID: 10861437.

[37] K. Oda, J. Hamanishi, K. Matsuo, K. Hasegawa, Genomics to immunotherapy of ovarian clear cell carcinoma: unique opportunities for management, Epub 2018/09/16, Gynecol. Oncol. 151 (2) (2018) 381–389, https://doi.org/10.1016/j.ygyno.2018.09.001. PubMed PMID: 30217369.

[38] B.M. Reid, J.B. Permuth, T.A. Sellers, Epidemiology of ovarian cancer: a review, Cancer Biol Med 14 (1) (2017) 9–32, https://doi.org/10.20892/j.issn.2095-3941.2016.0084. PubMed PMID: 28443200; PMCID: PMC5365187.

[39] K. Yamaguchi, M. Mandai, T. Oura, N. Matsumura, J. Hamanishi, T. Baba, S. Matsui, S.K. Murphy, I. Konishi, Identification of an ovarian clear cell carcinoma gene signature that reflects inherent disease biology and the carcinogenic processes, Epub 2010/01/12, Oncogene 29 (12) (2010) 1741–1752, https://doi.org/10.1038/onc.2009.470. PubMed PMID: 20062075.

[40] H. Matsushita, K. Hasegawa, K. Oda, S. Yamamoto, A. Nishijima, Y. Imai, K. Asada, Y. Ikeda, T. Karasaki, K. Fujiwara, H. Aburatani, K. Kakimi, The frequency of neoantigens per somatic mutation rather than overall mutational load or number of predicted neoantigens per se is a prognostic factor in ovarian clear cell carcinoma, Epub 2017/09/19, OncoImmunology 6 (8) (2017), e1338996, https://doi.org/10.1080/2162402X.2017.1338996. PubMed PMID: 28920005; PMCID: PMC5593715.

[41] B.C. Willis, E.A. Sloan, K.A. Atkins, M.H. Stoler, A.M. Mills, Mismatch repair status and PD-L1 expression in clear cell carcinomas of the ovary and endometrium, Epub 2017/07/29, Mod. Pathol. 30 (11) (2017) 1622–1632, https://doi.org/10.1038/modpathol.2017.67. PubMed PMID: 28752845.

[42] M.L. Friedlander, K. Russell, S. Millis, Z. Gatalica, R. Bender, A. Voss, Molecular profiling of clear cell ovarian cancers: identifying potential treatment targets for clinical trials, Epub 2016/03/05, Int. J. Gynecol. Cancer 26 (4) (2016) 648–654, https://doi.org/10.1097/IGC.0000000000000677. PubMed PMID: 26937756; PMCID: PMC4841290.

[43] B.E. Howitt, K.C. Strickland, L.M. Sholl, S. Rodig, L.L. Ritterhouse, D. Chowdhury, A.D. D'Andrea, U.A. Matulonis, P.A. Konstantinopoulos, Clear cell ovarian cancers with microsatellite instability: a unique subset of ovarian cancers with increased tumor-infiltrating lymphocytes and PD-1/PD-L1 expression, Epub 2017/03/28, OncoImmunology 6 (2) (2017), e1277308, https://doi.org/10.1080/2162402X.2016.1277308. PubMed PMID: 28344892; PMCID: PMC5353914.

[44] J. Hamanishi, M. Mandai, I. Konishi, Immune checkpoint inhibition in ovarian cancer, Epub 2016/04/09, Int. Immunol. 28 (7) (2016) 339–348, https://doi.org/10.1093/intimm/dxw020. PubMed PMID: 27055470.

[45] M.L. Disis, M.R. Patel, S. Pant, E.P. Hamilton, A.C. Lockhart, K. Kelly, J.T. Beck, M.S. Gordon, G.J. Weiss, M.H. Taylor, J. Chaves, A.C. Mita, K.M. Chin, Av Heydebreck, J.-M. Cuillerot, J.L. Gulley, Avelumab (MSB0010718C; anti-PD-L1) in patients with recurrent/refractory ovarian cancer from the JAVELIN Solid Tumor phase Ib trial: safety and clinical activity, J. Clin. Oncol. 34 (15_suppl) (2016) 5533, https://doi.org/10.1200/JCO.2016.34.15_suppl.5533.